

## Pseudo Fractal Tri-band Dipole Antenna For Mobile Wireless Sensors Networks

Catalin Popeanga\*. Radu Dobrescu.\*\*  
Gabriel Ionescu.\*\*\* Nicolai Christov\*\*\*\*

\*'Politehnica' University, Bucharest, Romania (e-mail: [catalin.popeanga@gmail.com](mailto:catalin.popeanga@gmail.com)).

\*\* 'Politehnica' University, Bucharest, Romania (e-mail: [rd\\_dobrescu@yahoo.com](mailto:rd_dobrescu@yahoo.com))

\*\*\* 'Politehnica' University, Bucharest, Romania (e-mail: [gion@clicknet.ro](mailto:gion@clicknet.ro))

\*\*\*\* University Lille 1, LAGIS, Lille, France (e-mail: [nicolai.christov@unv-lille1.fr](mailto:nicolai.christov@unv-lille1.fr))

---

**Abstract:** In today's research of wireless communications, there is increasing need for more compact, multi-band and moderate gain antennas for communications systems, for either military or commercial communications systems. Fractal antenna designs can meet these design requirements. This paper introduces a novel small size and multi-band fractal dipole antenna called pseudo fractal antenna where H tree fractal together with Fibonacci sequence build the main antenna body and the expected result is a tri-band antenna with resonance frequencies in the ISM bands 915Mhz, 2450Mhz and the 5800MHz. The performances of this pseudo fractal antenna were numerically analyzed with NEC2D professional software.

**Keywords:** Fractals, Antennas, Multi-band, Wireless sensors, Networks.

---

### 1. INTRODUCTION

The miniaturization of wireless sensor network requires the use of small, high-performance antennas that are normally one of the key components in determining the overall performance of a wireless sensor network. Conventional on-chip antenna, used in the present on the nodes, has a number of disadvantages in its current implementation including limited size, bandwidth (BW), efficiency and gain, thereby limiting the overall performance of the sensor node in different deployment scenarios.

It becomes extremely unproductive when the size of an antenna is made much smaller than the needed wavelength. The problem can be described rapidly as the reactive energy stored in antenna neighbourhood rapidly increases in the same time that the radiation resistance decreases, so both phenomena make these antennas difficult to match to the feeding circuit (Wemer (2000)). There are many solutions to solve this problem. A good way making miniature size antenna is using fractal geometry (Gianvittorio (2002)). In present days, the fractal antenna elements have drawn concerns of many antenna designers.

Mandelbrot (Falconer (1990)) defined fractals as a way of classifying complex geometric structures that have non-integer dimensions. While Euclidean geometries are limited to points, lines, areas and volumes of integer dimensions, fractal structures drop between these Euclidean classifications having non-integer dimension. Fractal geometries precisely describe many non-Euclidean features from nature, like coastlines, the branching of trees, the density of clouds. As an example: in case of cellular systems, not only the device antenna is important, but also those on

base stations. It is in this framework where fractal technology appears potentially as powerful tool to meet the telecommunication operator requirements (Wemer (2000)).

The relationship between the behaviour of an antenna and its size comparative to the wavelength has forced a tight constraint on the antenna designer. Conventional antennas are generally designed to operate at relatively narrow range of frequencies, typical approximately 10-40% around the centre wavelength. Moreover, there are minimum size limitations on conventional antennas as electrically small antennas are generally rather poor radiators.

Fractal antennas are becoming a useful method to design multi-band antennas with approximately the same input or radiation characteristics for different frequency bands. This results from the fact that most of the fractals are self-similar. The global fractal form is repeated at different sizes as many times as desired within the object structure such that the global object and its parts become similar. Fractals are space-filling curves; this implies that the wires lengths play a viable miniaturization technique.

The space filling, in two-dimensional systems, is called plane-filling, fractal type antennas revealed two significant benefits over the conventional antenna. The first advantage is that the increased electrical length leads to a lower resonant frequency, which effectively miniaturizes the antenna. The second advantage is that the enlarged electrical length can increase the input resistance of the antenna when it is used in a frequency range as a small antenna (Zainud-Deen (2004)). The theme treated in the following paragraphs targets the development of a low power radio architecture, which allowed design of antennas at much higher frequencies. The

antennas are investigated and designed for the frequencies of 915 MHz and 2.4 GHz, 5.8 GHz (Anjam (2006)). The scope is through proper selection of the feed and loading technique, gain power and size reduction compared with a normal dipole antenna can be achieved. Another important factor taken into account is that with every step in the miniaturization the resonance frequencies has to be in the specified base band.

### 2. ANTENNA FRACTAL MODEL

The proposed model is a combination of two well-known mathematical concepts, H-tree and Fibonacci sequence. In Fig. 1, the elements of H-tree fractal are graphically combined with segments defined by Fibonacci sequence. Consider the Fibonacci series:

$$F_n = F_{n-1} + F_{n-2} \tag{1}$$

The construction will start with  $F_1 = 1$  and  $F_2 = 1$ . The generated pseudo-fractal model starts with a segment of length  $len * \frac{1}{F_1}$ , 'len' is the initial length. In the next iteration, one end of the segment splits into two smaller segments of size  $len * \frac{1}{F_2}$ . Then at step n the segments are

split again in two smaller segments with size  $len * \frac{1}{F_n}$  and the process continue indefinitely. Since H-tree is based on a canopy tree fractal, it has to respect two conditions:

- the angle between any two connected segments has to be the same throughout the model. As it is defined the H-tree, the angle between any two connected segments from the same path is  $90^0$ .
- the ratio of lengths of any two consecutive line segments has to be constant as well. From the construction of the new model we have for two consecutive segments at step n the specific lengths  $len * \frac{1}{F_{n-1}}$  and  $len * \frac{1}{F_n}$ . This limit approaches the golden ratio (Knott (2011)). So, in our case:

$$\lim_{n \rightarrow \infty} \frac{\frac{1}{F_{n-1}}}{\frac{1}{F_n}} = \lim_{n \rightarrow \infty} \frac{F_n}{F_{n-1}} = \phi \tag{2}$$

The resulted model is presented in the Fig 1.

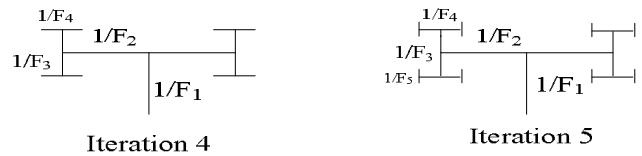
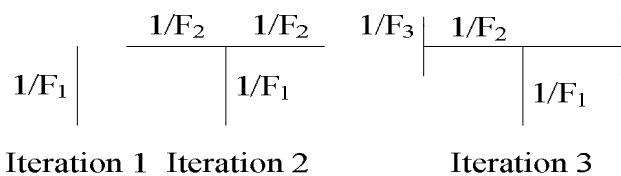


Fig. 1 5 iterations of the defined model

The obtained fractal has the Hausdorff dimension  $\frac{\log 2}{\log \phi}$ , the number of similarities between every stage increases by 2 because, at every step, every segment is split in two with the ratio calculated in equation (2).

In addition, every path in the fractal has the same length and this length is equal to

$$\sum_{n=1}^{\infty} \frac{len}{F_n} = len * \sum_{n=1}^{\infty} \frac{1}{F_n} \xrightarrow{n \rightarrow \infty} len * \psi \tag{3}$$

'1' is the initial length and  $\psi$  is reciprocal Fibonacci constant. The value of  $\psi$  is approximately 3.35988. The conclusion is that the built fractal occupies a rectangle with the perimeter no greater than

$$P = 2 * len * \psi \tag{4}$$

Moreover, the area is limited to

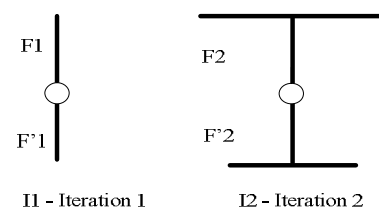
$$A = len^2 * \psi^2 \tag{5}$$

From (4) and (5) result that our antenna can be constructed on a finite area no matter how iterations are generated.

There are a few reasons behind the selection of this fractal and one is that the H-tree is used, a lot, in VLSI design as a clock distribution network for routing timing signals to all parts of a chip with equal transmission delays to each part (Burkis (1991)). For the same basis, the H-tree is used in micro-strip antennas in order to get the radio signal to every individual micro-strip antenna with equal propagation delay. Since our fractal is related with the H-tree, it will inherit this property.

### 3. ANTENNA GEOMETRY

The antenna will be generated from the defined fractal. To build a dipole antenna, the antenna will be composed of two fractals from the same generation but every fractal will have a different initial length 'l' and the feed element between these. As an example, the iteration I1 forms an asymmetrical dipole antenna, where each generation fractal is multiplied by its specific ratio I1 and I2. Five sequences of iterations of antenna are illustrated in Figure. 2.



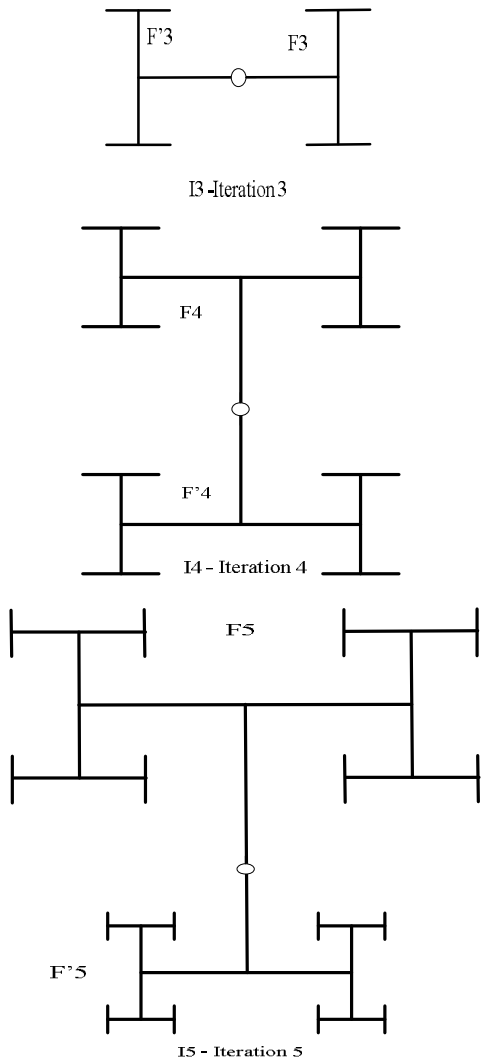


Fig. 2 Antenna Generations

Suppose  $F_i$  is the generated model at iteration  $i$  and  $(x_{0,i}, y_{0,i})$  is the starting point of each iteration,  $\theta$  is the angle of rotation and for our rotation it is  $180^\circ$ ,  $l'_i$  and  $l_i$  are the specific length and  $w$  is the feeding element and

$$F'_i = \frac{l'_i}{l_i} * \begin{bmatrix} 1 & 0 & 0 \\ 0 & 1 & 0 \\ 0 & 0 & 1 \end{bmatrix} \times \begin{bmatrix} 1 & 0 & x_{0,i} \\ 0 & 1 & y_{0,i} \\ 0 & 0 & 1 \end{bmatrix} \times \begin{bmatrix} \cos \theta & -\sin \theta & 0 \\ \sin \theta & \cos \theta & 0 \\ 0 & 0 & 1 \end{bmatrix} \times \begin{bmatrix} 1 & 0 & -x_{0,i} \\ 0 & 1 & -y_{0,i} \\ 0 & 0 & 1 \end{bmatrix} \times F_i, \tag{6}$$

then the antenna can be defined as  $I_i = \{F_i \cup F'_i \cup w\}$ .

#### 4. ANTENNA PARAMETERS

The most fundamental antenna parameters used in validating this type of antenna are:

- Impedance Bandwidth
- S-parameters
- Radiation pattern
- Efficiency
- Directivity
- Gain

All of the parameters mentioned are necessary to characterize an antenna, and to establish whether the antenna is optimized for its purpose.

##### 4.1 Impedance Bandwidth and S-parameters

The ‘impedance bandwidth’ describes the bandwidth over which the antenna has acceptable losses due to mismatch. The impedance bandwidth can be measured by the characterization of both the Standing Wave Ratio (SWR) and Return Loss (RL) at the frequency band of interest. The SWR is usually defined as a voltage ratio called the VSWR, for voltage standing wave ratio. SWR is used as an efficiency measure for transmission lines, electrical cables that conduct radio frequency signals, used for purposes such as connecting radio transmitters and receivers with their antennas. A problem with transmission lines is that impedance mismatches in the cable reflect the radio waves back toward the source, preventing the power from being diffused. SWR measures the relative size of these reflections. An ideal transmission line would have SWR equal to 1, with no reflected power back. An infinite SWR represents full reflection.

Both SWR (VSWR) and RL depend on measuring the reflection coefficient ( $\Gamma$ ).  $\Gamma$  is defined as the ratio of the amplitude of the reflected voltage wave ( $V_0^-$ ) normalized to the amplitude of the incident voltage wave ( $V_0^+$ ) at a load (David Pozar( 2005)).  $\Gamma$  can also be defined by using other field or circuit quantities and can be written as

$$\Gamma = \frac{V_0^-}{V_0^+} \tag{7}$$

The VSWR is defined as the ratio between the maximum voltage and minimum voltage of the standing wave created by the mismatch at the load on a transmission line

$$VSWR = \frac{1+|\Gamma|}{1-|\Gamma|} \tag{8}$$

$$RL = -20 \log |\Gamma| \text{ dB} \tag{9}$$

The scattering parameter S11 is equivalent to RL and is defined by the equation:

$$S_{11} = 20 \log |\Gamma| \text{ dB} \tag{10}$$

An acceptable mismatch for an antenna is normally 10% of the incident signal. This means the reflection coefficient  $\Gamma$  is equal to 0.31. For VSWR the impedance bandwidth lies between  $1 < VSWR < 2$ , and for Return Loss its value must be greater than 10dB or  $S_{11} < -10$  dB. Check the values in Fig. 3, Fig. 6, Fig. 9 and Fig. 12.

4.2 Radiation pattern

This is defined as “a mathematical function or a graphical representation of the radiation properties of the antenna as a function of space coordinates. In most cases, the radiation pattern is determined in the far-field region and is represented as a function of the directional coordinates. Radiation properties include power flux density, radiation intensity, field strength, directivity, phase or polarization.”(IEEE 2011)

The radiation pattern is the energy radiated relative to the antennas position. This is usually measured using spherical coordinates. For simulated parameters, see Fig. 5, Fig. 8, Fig. 11 and Fig. 14.

4.3 Antenna Efficiency, Directivity and Gain

All antennas suffer from losses. The antenna efficiency takes into account the losses at the input terminals and within the structure of the antenna while it is operating at a given frequency. The reflection efficiency ( $\eta_r$ ) is directly related to the return loss ( $\Gamma$ ):

$$\eta_r = 1 - |\Gamma|^2 \tag{11}$$

The radiated efficiency ( $\eta$ ) evaluates how much power is lost in the antenna because of conductor and dielectric losses:

$$\eta = \frac{P_{rad}}{P_{in}} \tag{12}$$

It is expressed as a percentage, where 100% (or 1.0) is perfectly lossless and 0% (or 0.0) is perfectly lousy.

Directivity measures the power density the antenna radiates in the direction of its strongest emission, in opposition to the power density radiated by an ideal isotropic radiator (which emits uniformly in all directions) radiating the same total power, where:

$U$  = radiation intensity (W/steradian)

$U_0$  = radiation intensity of an isotropic source (W/steradian)

$P_{rad}$  = radiated power (W).

$$D = \frac{U}{U_0} = \frac{4\pi U}{P_{rad}} \tag{13}$$

An isotropic radiator cannot be practically realized, the most comparable antenna is a short dipole, which has a directivity of 1.5. Any other antenna with a higher directivity than 1.5 is focused in a particular direction.

An antenna's power gain combines the antenna's directivity and electrical efficiency. As a transmitting antenna, this

element describes how well the antenna converts input power into radio waves headed in a specified direction. As a receiving antenna, it describes how well the antenna converts radio waves receiving from a specified direction into electrical power.

$$G = E_{antenna} * D \tag{14}$$

$$G_{dBi} = 10 \log_{10} G \tag{15}$$

The simulated results are shown in Fig. 4, Fig. 7, Fig. 10 and Fig. 13.

5. ANTENNA ANALYSIS

The analysis of studied antenna will begin with the most simple one generated in the first iteration, it is an asymmetrical dipole antenna, and we will continue to examine 4 iterations to see how the pseudo-fractal shape will influence the performances. The variable parameters are the initial length of the segments. In the last iteration, we will vary the diameter of the elements also. As it can be seen, in Table 1 the dimension of the coverage rectangle decreases.

Table .1 Dimensions of the antenna

I	$l_0$ (mm)	$l_1$ (mm)	Dimension on X (mm)	Dimension on Y (mm)
1	84	80	164	-
2	62	71	133	53
3	29	41	115	46
4	43	26	79	28
5	36	15	66	23

In practice, it is very hard to have the SWR between 1 and 2 and it is acceptable, also to have the values in the interval [2,4], and with the help of a radio tuning these can be adjusted. In the new transceivers this radio tuning is build-in. If the SWR values are far away from the ideal interval, some parameters can be changed: the diameter and the material of the line, resistance changes in the input stage. Another trick to have an acceptable SWR is to use micro strip antenna. Our model is very easy to use with it and one of the reasons is that the signal will travel the same length path for every partial antenna from the micro-stripes until the feed entrance. In the table 2 there are shown the simulated SWR for every studied antenna. As it can be seen, the minimization of the antenna does not have a great impact over the SWR parameter.

Table 2. SWR values

Iteration	SWR		
	915MHz	2450MHz	5800MHz
1	4.13	1.83	2.25
2	3.52	1.52	3.82
3	3.5	1.92	3.21

4	5.31	2.26	1.96
5	3.82	3.61	2.8

The antenna gain, Fig. 4, is much lower than the dipole antenna but it grows with next iteration, Fig. 7, Fig. 10, Fig. 13, proportional with the number of elements. The antenna gain can be set to a closer value of the dipole antenna if the diameters of the elements are changed to vary much more the resistance. For iterations 1 to 4, the diameter is constant and it is fixed to 0.5 mm. For the last iteration, the diameter varies to increase the gain of the antenna. The new diameters values will be for F0 fractal  $d_0 = 0.4$  mm and for F1  $d_1 = 1$  mm.

**Table 3. Antenna Gain**

Iteration	Gain(dBi)		
	915MHz	2450MHz	5800MHz
1	3.34	4.46	6.7
2	1.91	2.45	4.05
3	1.91	2.82	4.1
4	1.94	3.04	4.2
5	3.67	7.31	6.08

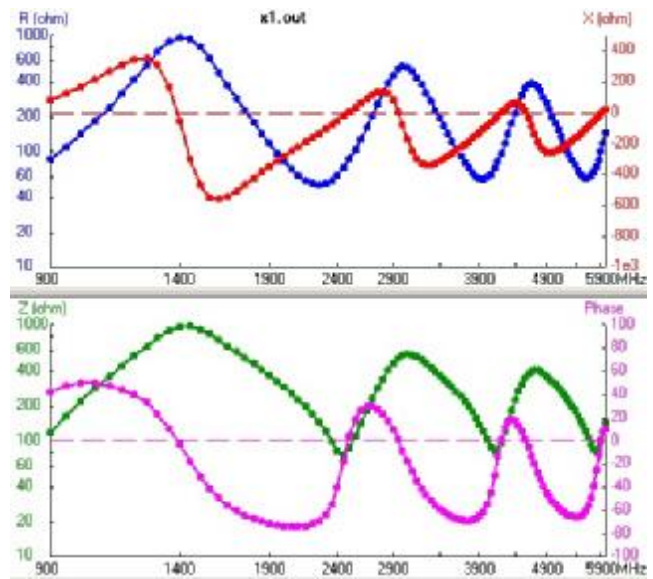
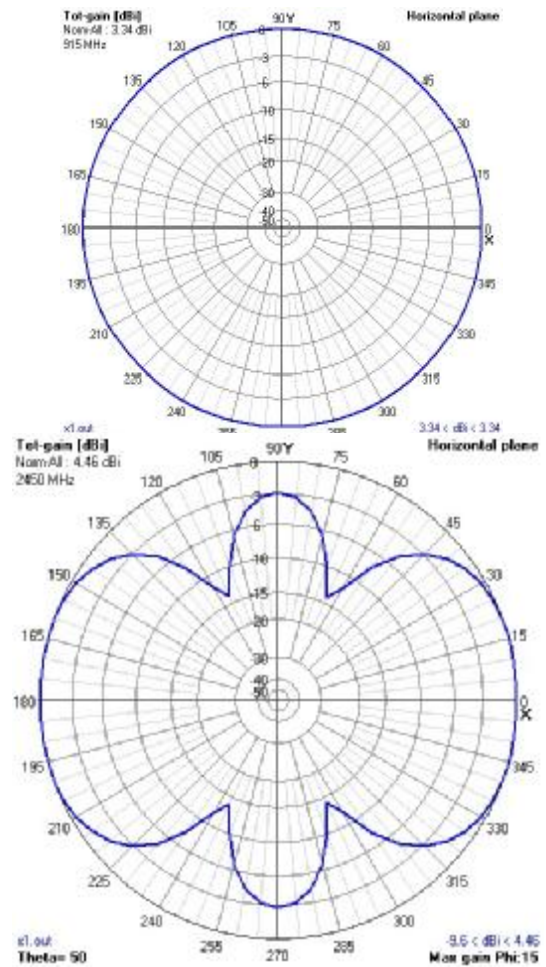
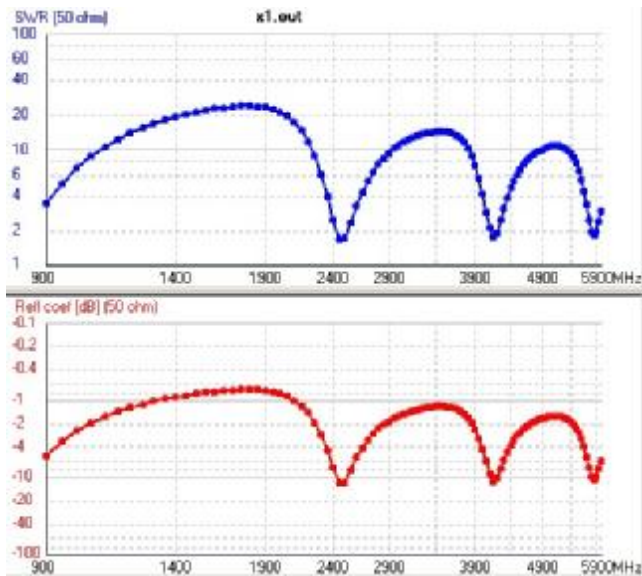


Fig. 3 Iteration 1 – SWR and Phase

6. ANTENNA SIMULATION

In the next figures, Fig.3 to Fig. 14, the antenna performances can be observed. In the SWR and phase figures, Fig. 3, Fig. 6, Fig. 9 and Fig. 12, in the specified frequency domain the multi band behaviour is graphically revealed. Starting from asymmetric dipole antenna, its behaviour begins to be close to a tri-band frequency. In addition, the resonance frequencies can be determined from these figures, Fig. 3, Fig. 6, Fig. 9 and Fig. 12. In the phase graphic where the red coloured line intersects the 0° degrees phase axe we will have the zeros for resonance.





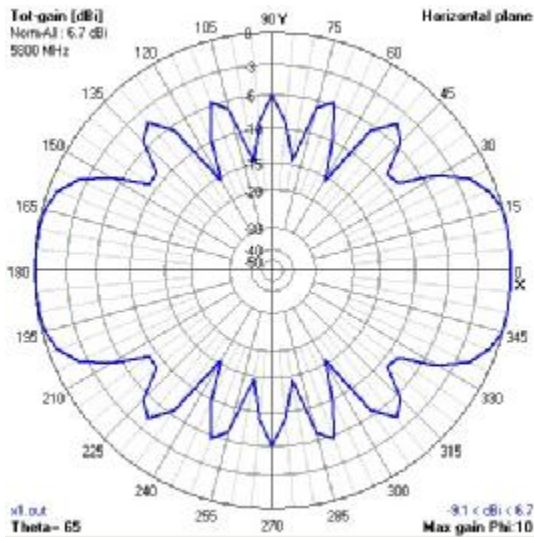


Fig. 4 Iteration 1 – Antenna Gain for the three radio bands

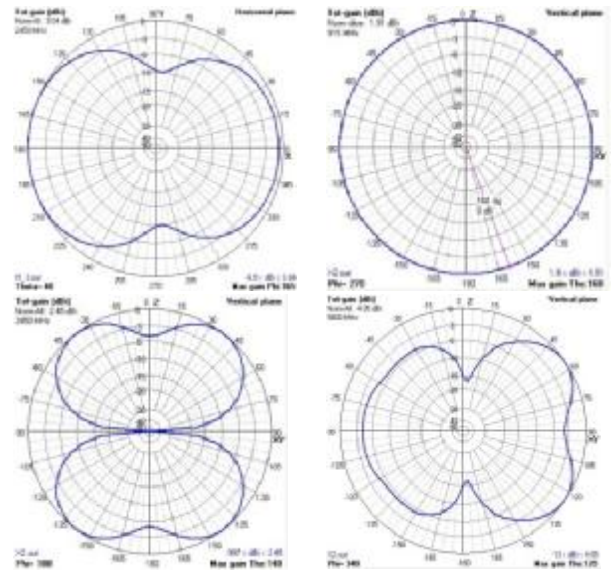


Fig. 7 Iteration 2 - Antenna Gain

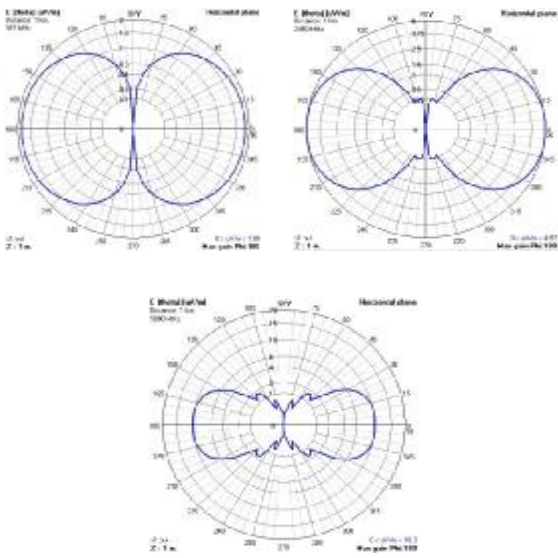


Fig. 5 Iteration 1 - Energy radiation at 1km distance

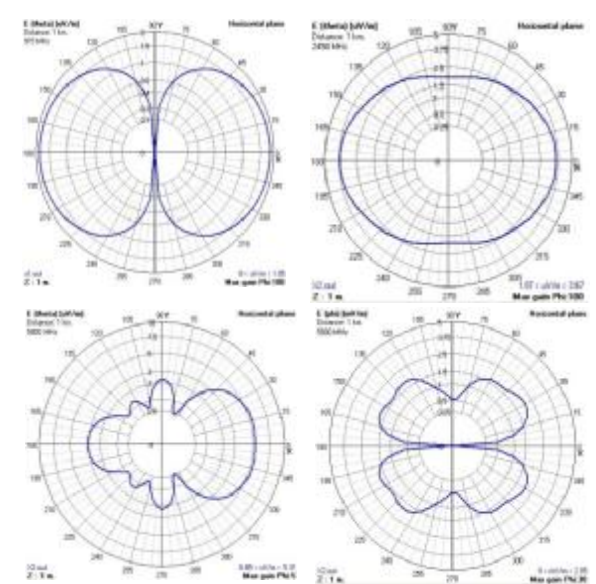


Fig. 8 Iteration 2 - Energy radiation at 1km distance

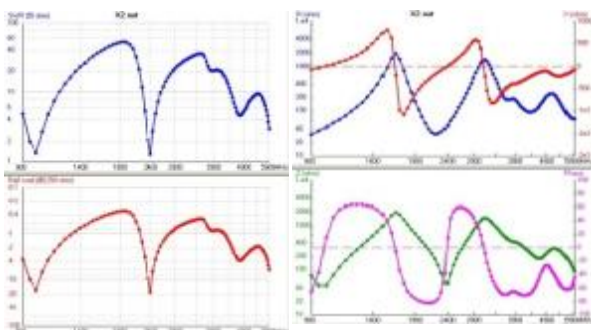


Fig. 6 Iteration 2 - SWR and phase

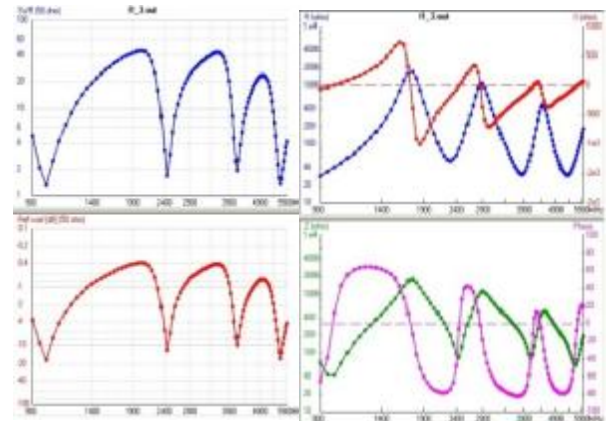


Fig. 9 Iteration 4 - SWR and phase

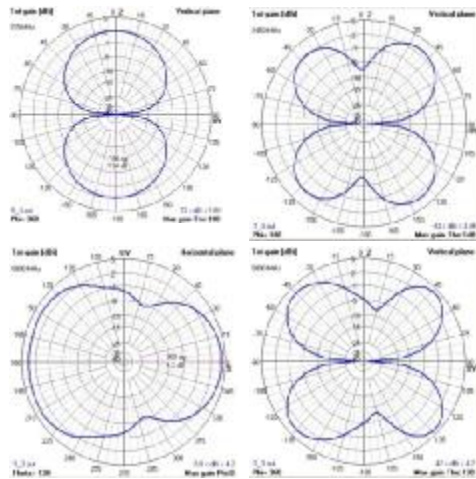


Fig. 10 Iteration 4 - Antenna Gain

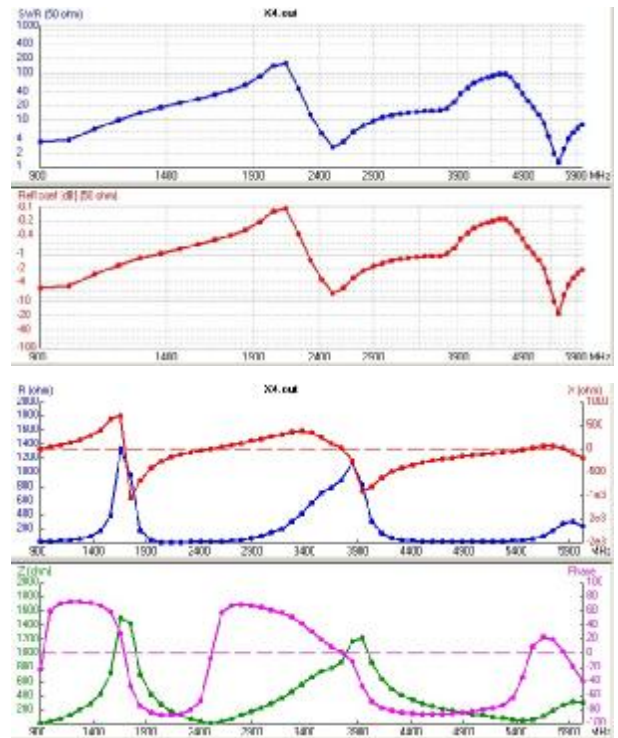


Fig. 12 Iteration 5 - SWR and phase

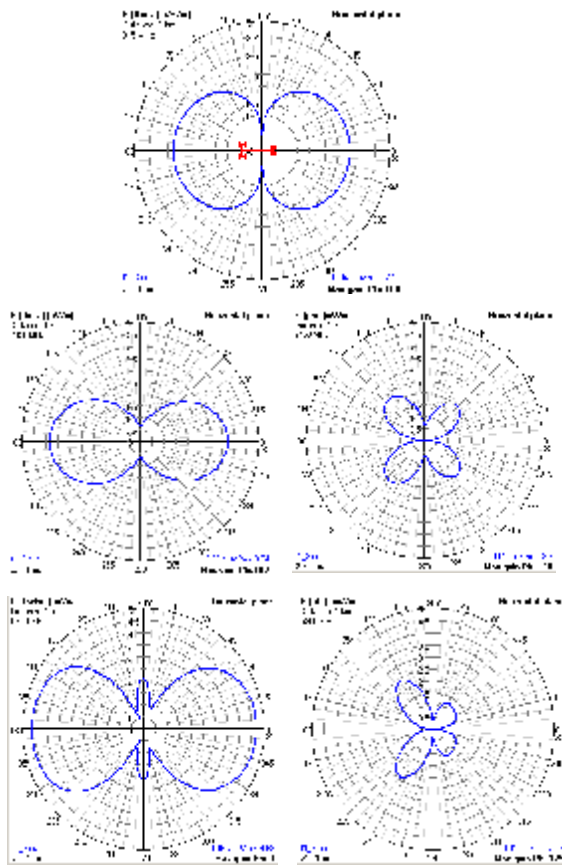


Fig. 11 Iteration 4 - Energy radiation at 1km distance

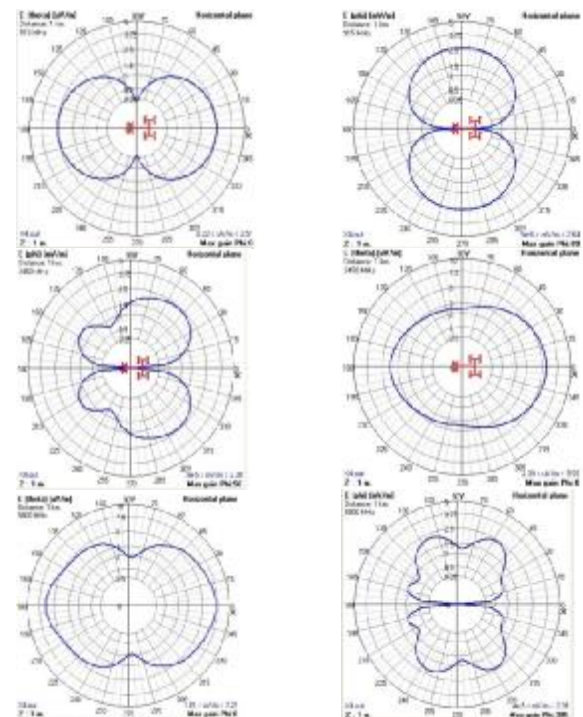


Fig. 13 Iteration 5 - Energy radiation at 1km distance



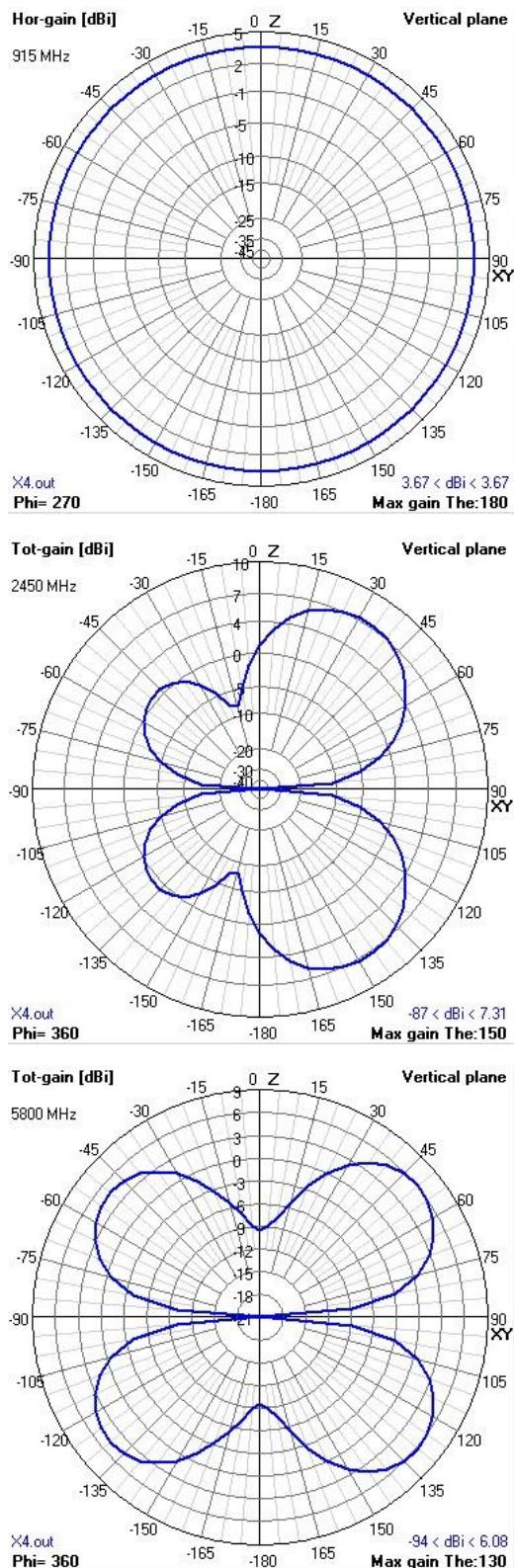


Fig. 14 Iteration 5 - Antenna Gain

## 7. CONCLUSION

The scope of the study is to propose a pseudo fractal antenna model to be a starting base for developing tri-band antenna for using in wireless sensors networks in the ISM bands 915MHz, 2450MHz and 5800MHz. Another important factor taken into account was that with every step in the minimization the resonance frequencies remain, in an acceptable interval, the same. The preserve of resonance frequencies is a different way to study the performance of fractal antenna as it was studied before (Waqas (2009), Yan (2008)). This pseudo-fractal antenna holds multi-band, in particular tri-band, behavior similar to other pseudo-fractal antenna like Sierpinski gasket antenna or hexagonal fractal antenna. This new pseudo-fractal antenna allows flexibility in matching tri-band operations in which larger frequency separation is needed. The simulated results show a good energy radiation structure, with almost the same directivity and gain, when compared to a frequency specific dipole antenna. The SWR measurements show that this type of antenna can be used successfully in the free ISM bands for developing wireless sensors networks.

## REFERENCES

- Anjam RiazI & Maaruf. (2006). Fractal Antenna and their Multi-band Performance Evaluation, Applied Electronics, pp 11-14, *IEEE, Pilsen*.
- Burkis, J. (1991). Clock tree synthesis for high performance ASICs, IEEE International Conference on ASIC, Proceeding, Fourth *Annual IEEE International*, IEEE, Rochester, NY, vol 9, pp 1-3.
- David M. Pozar. (2005). Microwave Engineering, *John Wiley & Sons*, Amherst US.
- Gianvittorio J. P. and Y. Rahmat-Sanmi. (2002). Fractal Antennas: A Novel Antenna Miniaturization Technique and Applications. *IEEE Antennas & Propagation Magazine*, vol. 44, no. 1, pp 20-36.
- Falconer K. (1990). Fractal geometry: mathematical foundation and applications. *John Wiley & Sons*, England.
- IEEE. (2011). IEEE Standard Definitions of Terms for Antennas, IEEE Transactions on Antennas and Propagation, US.
- Knott R. (2011). Fibonacci Numbers and the Golden Section. <http://www.mcs.surrey.ac.uk/Personal/R.Knott/Fibonacci>.
- Waqas, M., Z. Ahmad, and M. Ihsan. (2009). Multiband Sierpinski fractal antenna. Proc. *IEEE International Multitopic Conference (INMIC 2009)*, pp. 376-381, Pakistan.
- Wemer D. H. and R. Mitra. (2000). Frontiers in Electromagnetics. *Wiley-IEEE Press*, US.
- Yan Su, Xiao-Zheng Lai. (2008). Research on Fractal Tree RFID Tag Antenna. *Wireless Communications, Networking and Mobile Computing*, pp 1-3.
- Zainud-Deen S.H, Awadalla. (2004). Radiation and Scattering from Koch Fractal Antennas. Radio Science Conference, 2004. NRSC 2004. *Proceedings of the Twenty-First National*, vol. B8, pp 1-9.